diversity

MDPI

Article

Fragilaria shirshovii sp. nov.—A New Species of Araphid Diatoms (Bacillariophyta, Fragilariophyceae) from the Gulf of Ob (Kara Sea, Arctic)

Nikolay V. Lobus [1,*], Anton M. Glushchenko [1,*], Sergei I. Genkal [2], Yevhen I. Maltsev [1] and Maxim S. Kulikovskiy [1]

[1] Timiryazev Institute of Plant Physiology, Russian Academy of Sciences, 35 Botanicheskaya St., 127276 Moscow, Russia
[2] Papanin Institute for Biology of Inland Waters, Russian Academy of Sciences, 152742 Borok, Russia
* Correspondence: lobus.nikolay@gmail.com (N.V.L.); closterium7@gmail.com (A.M.G.)

Abstract: A new species, *Fragilaria shirshovii* sp. nov., is described on the basis of molecular and morphological investigations. Cells were isolated from the surface levels of desalinated water masses in the zone of mixing river and marine waters in the Gulf of Ob. The morphology of this species is analyzed with light microscopy (LM) and scanning electron microscopy (SEM). The valves of *F. shirshovii* sp. nov. are fusiform to almost linear. The frustules are linked together in the central part, forming double comb-shaped colonies. The axial area is narrow and linear, with a distinct rounded or rectangular fascia in the center. Ghost striae are present on the central area. Areolae are not discernible in LM. Apical pore fields are composed of small pores and closed papillary outgrowths. The lips of the rimoportula are well pronounced and the striae are uniseriate. Phylogenetic analysis based on partials 18S rRNA and *rbc*L genes infers the species *F. shirshovii* sp. nov. as a member of Fragilariaceae. The species most resembling F. *shirshovii* sp. nov. are *F. crotonensis*, *F. pararumpens*, *F. bidens* and *F. perminuta*. The differences between *F. shirshovii* sp. nov. and close taxa are discussed. This work is a pioneer investigation of Fragilariaceae taxa from the freshwater ecosystems of the Siberian Arctic using a combination of morphological and molecular tools.

Keywords: diatoms; morphology; taxonomy; phylogeny; *rbc*L; SSU; Western Siberia

Citation: Lobus, N.V.; Glushchenko, A.M.; Genkal, S.I.; Maltsev, Y.I.; Kulikovskiy, M.S. *Fragilaria shirshovii* sp. nov.—A New Species of Araphid Diatoms (Bacillariophyta, Fragilariophyceae) from the Gulf of Ob (Kara Sea, Arctic). *Diversity* **2023**, *15*, 916. https://doi.org/10.3390/d15080916

Academic Editors: Małgorzata Poniewozik and Bert W. Hoeksema

Received: 26 April 2023
Revised: 18 July 2023
Accepted: 4 August 2023
Published: 7 August 2023

1. Introduction

Arctic ecosystems are the most sensitive to global climate change. The environmental transformation that happens in the Arctic Region is largely determined by the processes occurring in the estuaries of the largest Siberian Rivers [1,2]. In addition, Arctic ecosystems are particularly sensitive to anthropogenic stresses associated with both human activities in the seas and pollutants from river runoff [3,4]. The great biogeographic and conservation importance of the Arctic is confirmed by the peculiar climatic characteristics and complex paleogeographic and paleoclimatic history of the region, combined with the high diversity of environmental conditions [5–7].

Diatoms are the most diverse groups of microalgae, occurring in a wide variety of aquatic ecosystems, where they can be excellent indicators of environmental features in the changing climate and growing anthropogenic load [8,9]. They are sensitive to changes in environmental conditions, and the diatom community (type of diatom species and their relative abundance) in a river is largely influenced by the surrounding water quality [10]. However, it is critical to separate different species from each other because they can provide different ecological information [11–13].

The genus *Fragilaria* Lyngbye 1819 is distributed throughout the world in different climatic zones. It is often an important part of microalgae communities in freshwater ecosystems on a wide spectrum of environmental conditions [14–17]. The *Fragilaria* taxa

are present in both oligotrophic and eutrophic conditions and have varying preferences for pH, from acidophilic to alkaliphilic. There are also variations in life forms. The *Fragilaria* species mostly form colonies, however some live as single cells. Many of these taxa are benthic, but some are planktonic [18].

Currently, it is universally acknowledged that delineating species in the genus *Fragilaria* is a fairly complicated task [19]. Despite many studies that were carried out in the last two decades, the issues of identification, species delineation and the revision of the genus *Fragilaria* are still unresolved [15,16]. Generally, this can be explained by the shared morphological traits between species, species descriptions that are based solely on light microscopy, as well as the overlapping values of quantitative traits and the necessity of using SEM to document taxonomically important features [18].

The aim of this study is to describe a new species of *Fragilaria*, isolated from the desalinated waters of the Gulf of Ob. This work is the first study of the genus *Fragilaria* from freshwater ecosystems of the Siberian Arctic that uses a combination of morphological and molecular tools, which will allow us to contribute to the understanding of the biodiversity and ecological plasticity of this group. In addition, this will enable future improvements of modern approaches and methods of environmental monitoring and environmental quality assessments based on diatom analysis.

2. Materials and Methods

2.1. Study Area and Environmental Conditions

The Gulf of Ob is located in the southern part of the Kara Sea in the Arctic Ocean and is one of the largest estuaries in the World Ocean (Figure 1). The Gulf of Ob has a length of 850 km and annually receives approximately 530 km^3 of freshwater river runoff. The Ob River has a long freshet from May–June to August–September (20,000–40,000 m^3/s). This period accounts for about 80% of the total annual freshwater runoff. The southern and central parts of the Gulf of Ob are freshwater during the entire year [20,21].

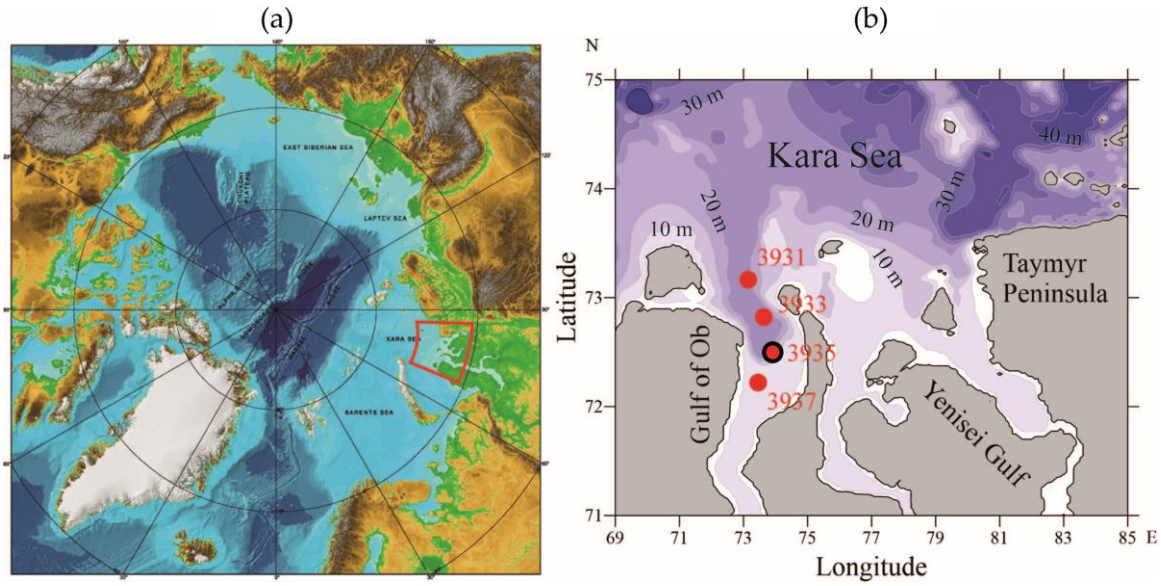

Figure 1. (**a**) IBCAO map of the Arctic Ocean; the red contour indicates the area of the field survey performed in the Kara Sea. (**b**) Bathymetry of the southern part of the Kara Sea; red circle with black contour indicates location of water sampling site in the Gulf of Ob (station no. 3935).

The vertical temperature and salinity structure observed along the transect in the Gulf of Ob in August 2021 are shown in Figure 2. A typical two-layered structure of the water masses is observed in the estuary with a low-saline (<15 PSU) and warm (>7 °C) surface layer and a saline (>25 PSU) and cold (<3 °C) bottom layer, with a sharp vertical gradient at their interface [22].

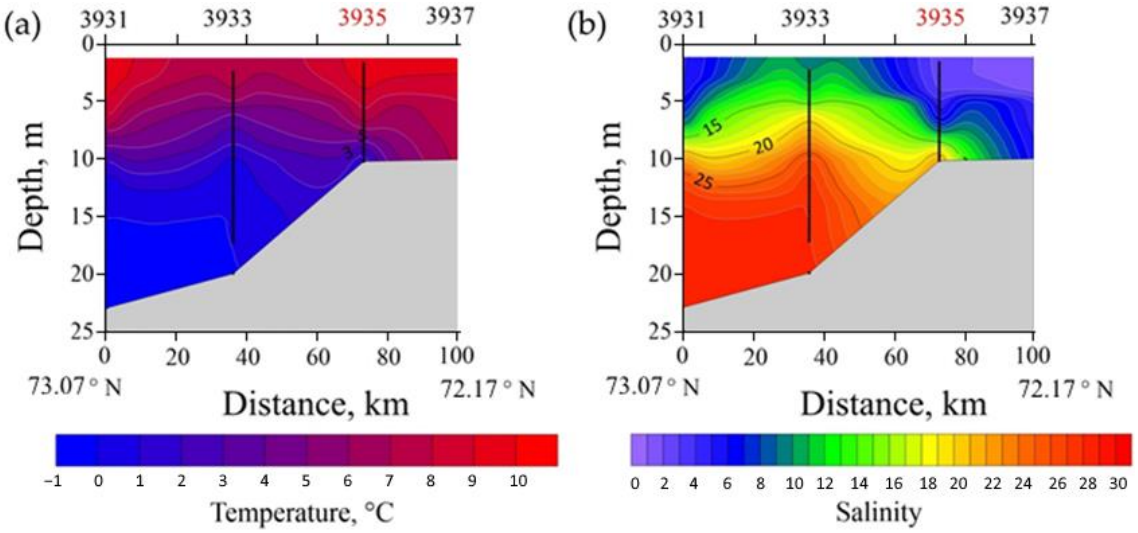

Figure 2. The vertical temperature (**a**) and salinity (**b**) structure along the transect in the Gulf of Ob on 15–16 August 2021. Water sample analyzed in this study was collected at station 3935 (indicated by red color) [22].

The southernmost stations (st. 3935, 3937) at transect were located in a river-dominated shallow area (10–12 m deep) with salinity equal to 0–2 from surface to bottom. Further northward, the depth increases, and the freshened surface layer separates from the bottom and overlies the landward inflow of saline seawater (Figure 2). The vertical thermohaline structure along the transect in the Gulf of Ob was variable due to the meandering of the main seaward flow of freshened water within the estuary [21].

The hydrochemical structure of the water masses across the gulf–coastal zone–open sea gradient was strongly influenced by river runoff. In the desalinated part of the Gulf of Ob, the concentrations of nutrients and dissolved silica were usually relatively high. In the southern and central parts of the Gulf of Ob, the algal community was represented by a freshwater complex of species, which were brought by river runoff. The maximum values of primary production in the estuary, as well as on the adjacent shelf of the Kara Sea, were confined to the surface layer of the water column [17,23].

2.2. Sample Collection

Sampling was carried out in the Gulf of Ob during the 58th voyage of the RV "Akademik Ioffe" to 15–16th of August 2021 under the program "Arctic Floating University". Water samples were collected in the topmost layer of water (0.5–1.0 m) with the sampling system "Rosetta", with attached plastic Niskin bottles on station 3935 (72°28.636′ N, 73°56.701′ E) (Figures 1 and 2). The samples were then deposited in sterile polypropylene containers and stored in a cool light place until the culturing process in the laboratory. The hydrochemical conditions during the sampling were the following: t = 10.65 °C, pH = 8.17 and salinity < 0.1 PSU [22].

2.3. Diatom Strain Isolation and Culturing

The monoclonal unialgal culture of this strain was established by micropipetting cells under an inverted microscope. Separate cells from the water sample were transferred with a micropipette onto a slide and washed several times with sterile water. Afterwards, the cells were transferred with a clean glass micropipette into immunological microplates with liquid culturing medium WC [24]. The plates were wrapped with Parafilm® and stored in a lightbox at a temperature of 22–25 °C and a photoperiod light/dark of 16:8 h. After 10–14 days, separate algal colonies unaffected by fungi were carefully transferred to a Petri dish with sterile culture medium. The Petri dish was wrapped in Parafilm® and stored in a lightbox with a temperature of 8–10 °C and the same photoperiod of 16:8 h [25].

In order to acquire the necessary amount of biomass, the cells of this strain were grown in 120 mL glass flasks containing 40 mL of the WC culturing medium. Initially, 1 mL of inoculum was added to each flask. Before culturing, the WC medium was sterilized in an autoclave, and after cooling, the pH was brought to 7.0–7.2. The starting concentration of cells in the medium was 10^3 cells ml^{-1}. The flasks were incubated by white fluorescent light of 100 µmol PAR photons m^{-2} s^{-1} with the photoperiod light/darkness of 16:8 h, while constantly shaking on an orbital shaker (120 rpm). The culturing was carried out at a temperature of 22 ± 0.5 °C until reaching the stationary growth phase [22].

2.4. Preparation of Slides and Microscope Investigation

In order to remove organic matter, the diatom cell culture in the stationary growth phase was concentrated and then boiled in H_2O_2 (≈37%) for 6 h. After cooling, the sample was concentrated once more and washed with distilled water 4 times at 12-h intervals. Afterwards, the suspension was spread onto coverslips and dried on an electric hot plate. The material was mounted in Naphrax™ (Brunel Microscopes Ltd., Chippenham, UK; refractive index = 1.73). Light microscopy (LM) was carried out using a Zeiss Scope A1 microscope (Carl Zeiss Microscopy GmbH, Göttingen, Germany), equipped with a Zeiss oil immersion objective (100×/n.a.1.4, Nomarski differential interference contrast) and a Zeiss Axio-Cam ERc 5s camera (Carl Zeiss NTS Ltd., Oberkochen, Germany). Scanning electron microscopy (SEM) was used to study the valve ultrastructure. To prepare for SEM, diatom valve suspension was spread onto aluminum stubs that were 10 mm in diameter and dried at room temperature. The stubs were sputter-coated with 50 nm of Au by means of an Eiko IB 3 (Eiko Engineering, Yamazaki, Hitachinaka Shi, Ibaraki Ken, Japan). Valve ultrastructure was examined in the Papanin Institute for Biology of Inland Waters RAS, Borok, Russia, with a JSM-6510LV scanning electron microscope (JEOL Ltd., Tokyo, Japan) with an accelerating voltage of 10 kV and operating distance of 11 mm and JSM-6060A (JEOL Ltd., Tokyo, Japan) scanning electron microscope operated at 10 kV and 11-mm distance, in the Laboratory of Structural and Morphological Research, Frumkin Institute of Physical Chemistry and Electrochemistry, Russian Academy of Sciences (Moscow, Russia). The cleaned samples, slides and stubs are stored in the Laboratory of molecular systematics of aquatic plants, Timiryazev Institute of Plant Physiology, RAS (Moscow, Russia) [22].

2.5. Molecular Analyses

Total DNA from the studied strains was extracted using Chelex 100 Chelating Resin, molecular biology grade (Bio-Rad Laboratories, Hercules, CA, USA). According to the manufacturer's protocol, 2.2. Partial 18S rDNA fragment (390 bp, including the highly variable V4 region of the 18S rRNA gene) of diatom strain ARC 03 was amplified using primers D512for and D978rev [26]. Partial *rbc*L plastid gene fragment (1014 bp) was amplified using primers rbcL404+ [27] and dp7 [28].

Amplifications were carried out using premade polymerase chain reaction (PCR) mastermixes (ScreenMix by Evrogen, Moscow, Russia). The amplification conditions for the V4 region were as follows: initial denaturation for 5 min at 95 °C, followed by 35 cycles of 30 s of denaturation at 94 °C; 30 s of annealing at 52 °C; and 50 s of extension at 72 °C, with the final extension for 10 min at 72 °C. The amplification conditions for the *rbc*L gene were as follows: initial denaturation for 5 min at 95 °C, followed by 45 cycles of 30 s of denaturation at 94 °C; 30 s of annealing at 59 °C; and 80 s of extension at 72 °C, with the final extension for 10 min at 72 °C. PCR products were visualized by horizontal electrophoresis in 1.0% of agarose gel stained with SYBRTM Safe (Life Technologies, Waltham, MA, USA). The products were purified with a mixture of FastAP, 10 × FastAP Buffer and Exonuclease I (Thermo Fisher Scientific, Waltham, MA, USA) in aqueous solution. Sequencing was performed using a Genetic Analyzer 3500 instrument (Applied Biosystems, St. Louis, MO, USA).

The editing and assembling of the consensus sequences were carried out by processing the direct and reverse chromatograms in Ridom TraceEdit ver. 1.1.0 (Ridom GmbH, Mün-

ster, Germany) and Mega ver. 7 software [29]. The reads were included in the alignments along with corresponding sequences of 34 diatom algae species downloaded from GenBank. Two species of centric diatoms (*Stephanodiscus minutulus* and *Stephanodiscus hantzschii*) were chosen as outgroup taxa (taxa names and Accession Numbers are provided in Figure 3).

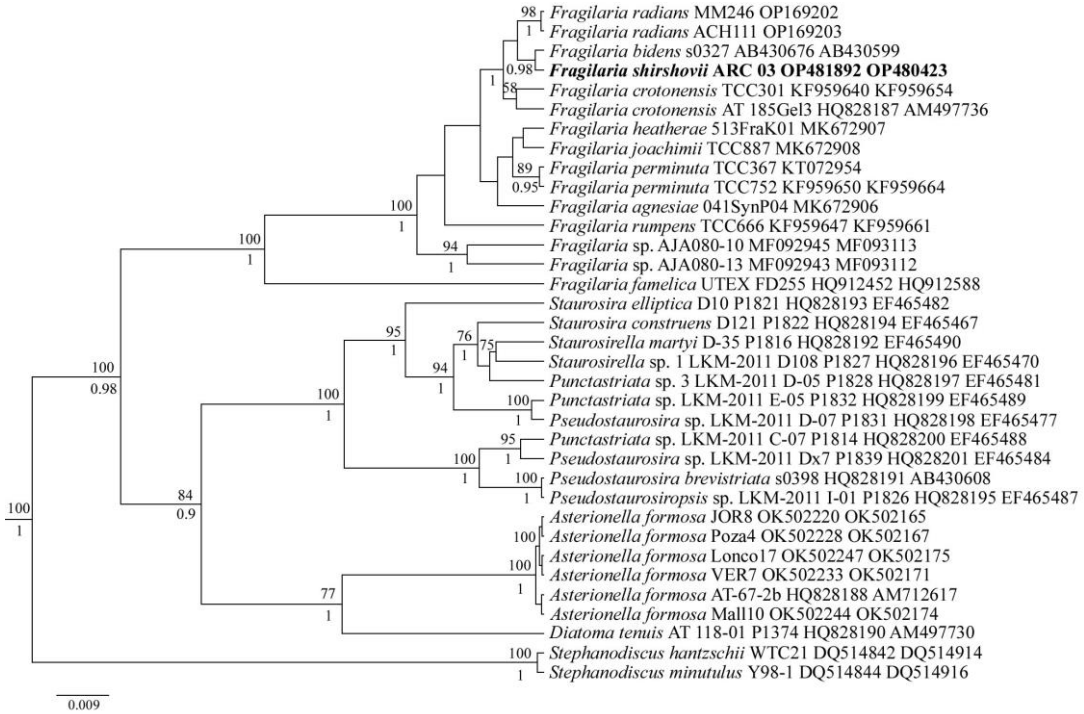

Figure 3. Phylogenetic position of *Fragilaria shirshovii* ARC 03 (indicated in bold) based on Bayesian inference for the partial *rbc*L and 18S rDNA genes. Total length of the alignment is 1375 characters. Values above the horizontal lines are bootstrap support from RAxML analyses (<50 are not shown) and values below the horizontal lines are Bayesian posterior probabilities (<90 are not shown). Strain numbers (if available) and GenBank numbers are indicated for all sequences. Species from the centric diatoms were used as an outgroup.

The nucleotide sequences of the 18S rRNA and *rbc*L genes were aligned separately using the Mafft v7 software and E-INS-i model [30]. The final alignments were carried out by a procedure whereby unpaired sites were visually determined and removed from the beginning and end of the resulting matrices. For the protein-coding sequences of the *rbc*L gene, it was checked if the beginning of the aligned matrix corresponded to the first position of the codon (triplet). The resulting alignments had lengths of 421 (18S rDNA) and 954 (*rbc*L) characters. After the removal of the unpaired regions, the aligned 18S rDNA gene sequences were combined with the *rbc*L gene sequences into a single matrix.

The data set was analyzed using the Bayesian inference (BI) method implemented in Beast ver. 1.10.1 software [31] to construct a phylogeny. For the alignment partition (most appropriate substitution model), shape parameter α and a proportion of invariable sites (pinvar) were estimated using the Bayesian information criterion (BIC), as implemented in jModelTest 2.1.10 [32].

This BIC-based model selection procedure selected the following models, shape parameter α and a proportion of invariable sites (pinvar): TrN + G, α = 0.3010 for 18S rDNA; F81 + I, pinvar = 0.8340 for the first codon position of the *rbc*L gene; JC + I + G, α = 0.6090 and pinvar = 0.8700 for the second codon position of the *rbc*L gene; and TPM3uf + G, α = 0.6260 for the third codon position of the *rbc*L gene. We used the HKY model of nucleotide substitution instead of TrN, the F81 model of nucleotide substitution instead of JC, and the GTR model instead of TPM3uf, given that they were the best matching models available for BI. A Yule process tree was used prior as a speciation model for all phylo-

genetic reconstructions. The analysis ran for 5 million generations, with chain sampling occurring every 1000 generations. The parameters-estimated convergence, effective sample size (ESS) and burn-in period were checked using Tracer ver. 1.7.1 software (MCMC Trace Analysis Tool, Edinburgh, United Kingdom) [31]. The initial 25% of the trees were removed, and the rest were retained to reconstruct a final phylogeny. The phylogenetic tree and posterior probabilities of its branching were obtained on the basis of the remaining trees having (see Section 4) estimates of the parameter models of nucleotide substitutions and likelihood. The Maximum Likelihood (ML) analysis was performed using the RAxML program [33]. Nonparametric bootstrap analysis with 1000 replicas was used. FigTree ver. 1.4.4 (University of Edinburgh, Edinburgh, United Kingdom) and Adobe Photoshop CC ver. 19.0 soft-ware (Adobe, San Jose, CA, USA) were used for visualizing and editing the trees.

3. Results

3.1. Morphological Analysis

For the morphological description of species in this article, we used the terminology by [12,14,15,18,34–36].

Fragilaria shirshovii Glushchenko and Kulikovskiy sp. nov. (Figures 4–7).

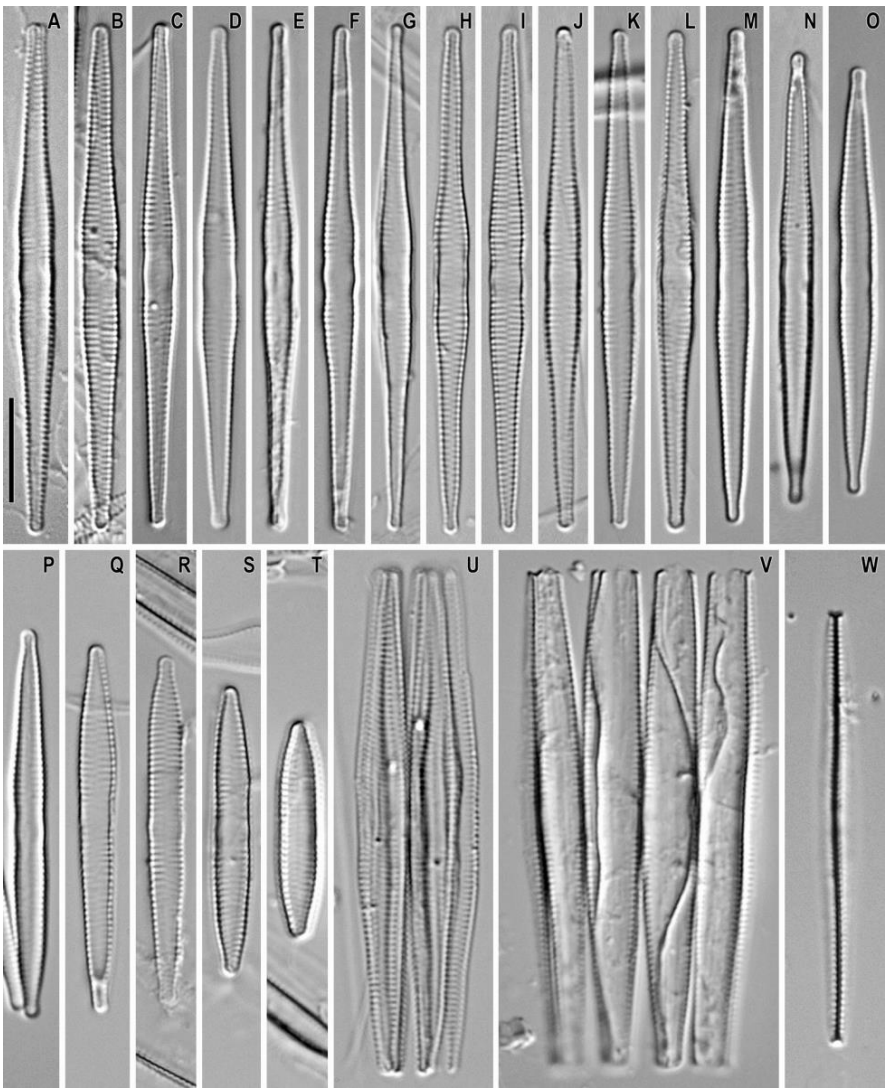

Figure 4. (**A**–**W**). *Fragilaria shirshovii* Glushchenko and Kulikovskiy sp. nov. Strain ARC 03. Slide no. 08440a. Light microscopy, differential interference contrast. Oxidized material. (**A**–**T**). Valve face, size diminution series. (**U**,**V**). Frustules in girdle view, double comb-shaped colonies. (**W**). Structure in the form of two connected valves of different cells. (**F**). Holotype. Scale bar = 10 μm.

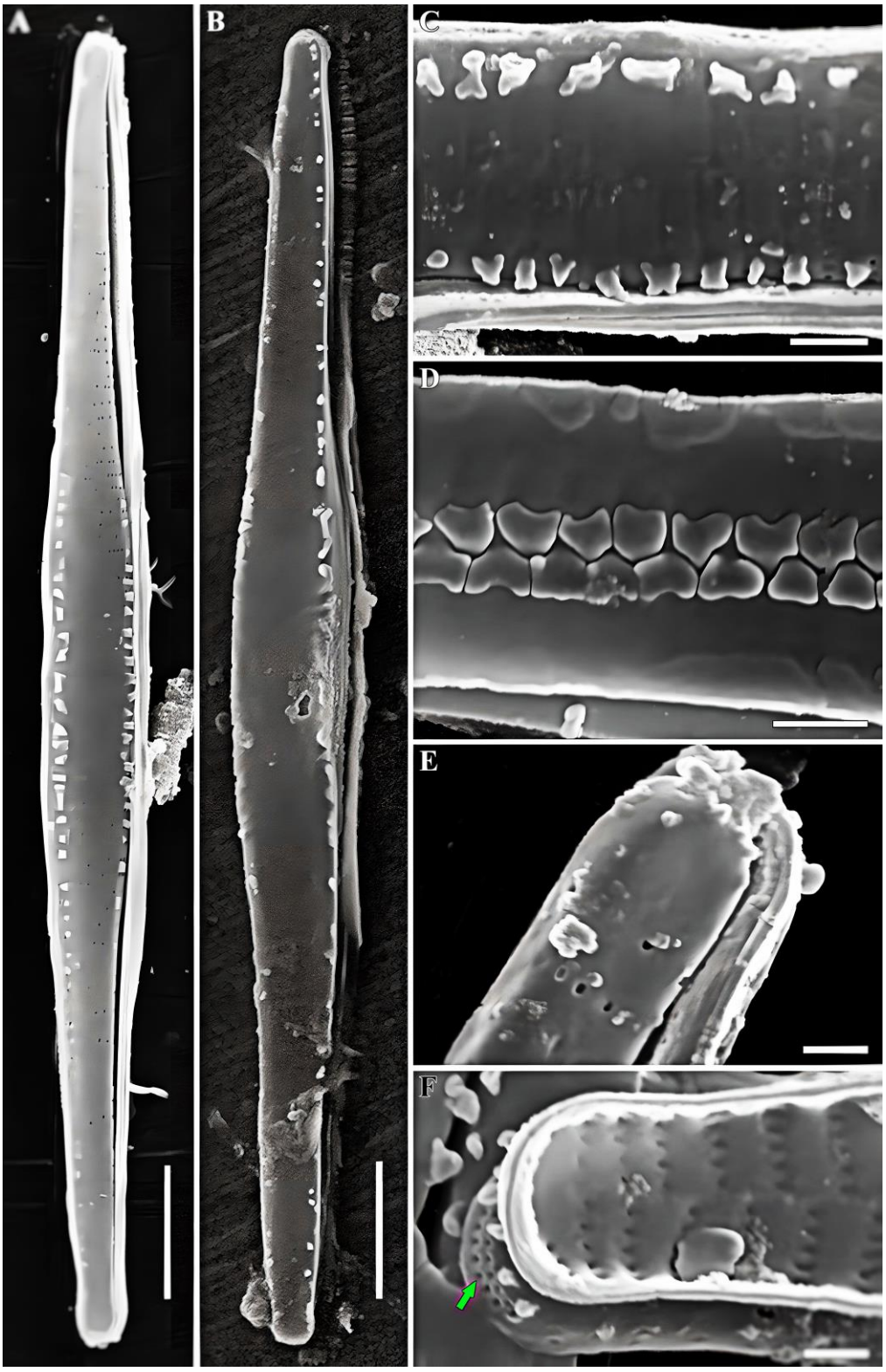

Figure 5. (**A**–**F**). *Fragilaria shirshovii* Glushchenko and Kulikovskiy sp. nov. Strain ARC 03. Scanning electron microscopy, external views. (**A**,**B**). The whole valve. (**C**). Central area. (**D**). Two valves of different frustule connect by spatula-shaped spines. (**E**). Valve end. (**F**). Green arrow shows the apical pore field. Scale bars (**A**,**B**) = 5 μm; (**C**,**D**) = 1 μm; (**E**,**F**) = 0.5 μm.

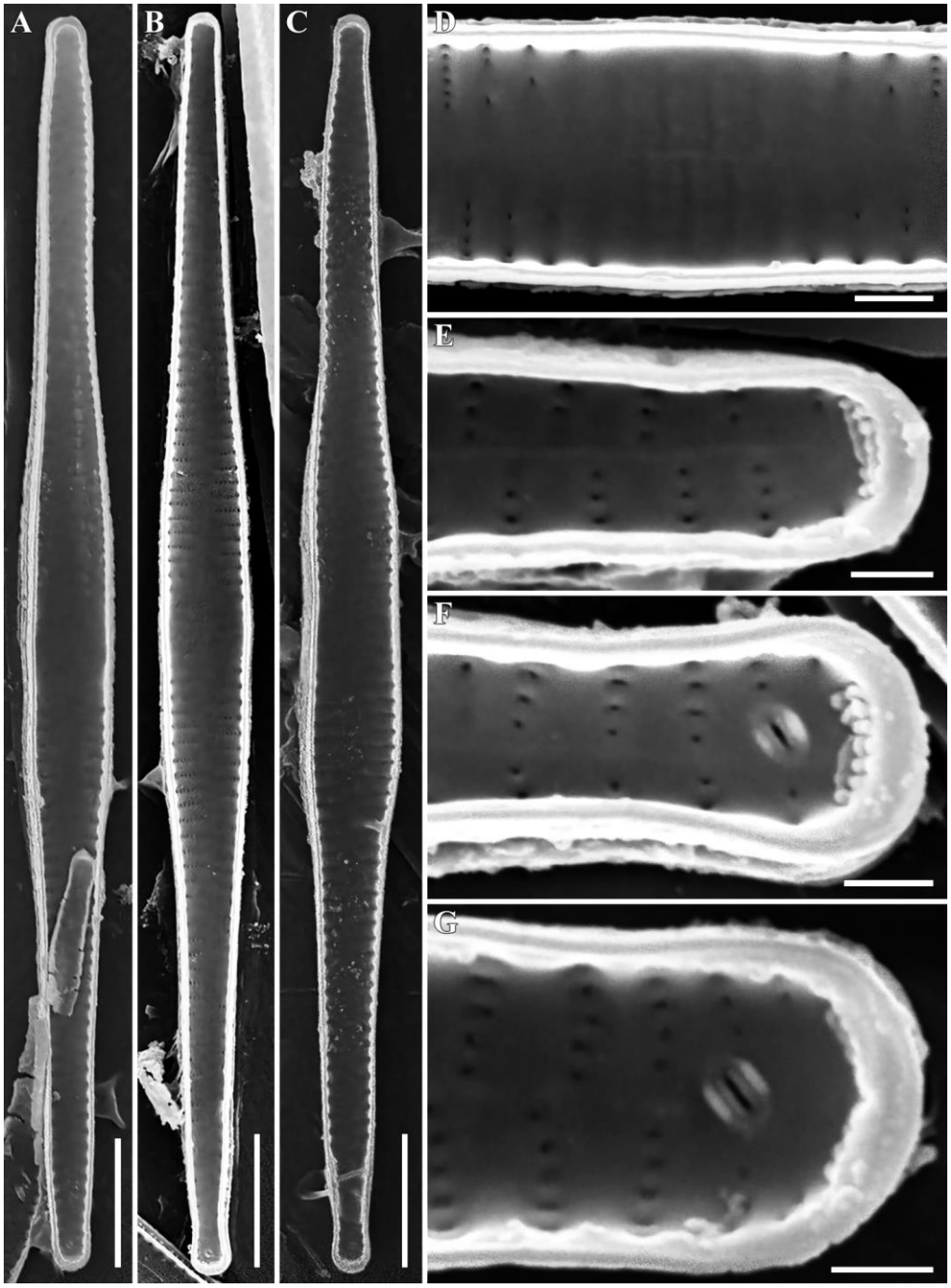

Figure 6. (**A**–**G**). *Fragilaria shirshovii* Glushchenko and Kulikovskiy sp. nov. Strain ARC 03. Scanning electron microscopy, internal views. (**A**–**C**). The whole valve. (**D**). Central area. (**E**–**G**). Valve ends. Scale bars (**A**–**C**) = 5 μm; (**D**) = 1 μm; (**E**–**G**) = 0.5 μm.

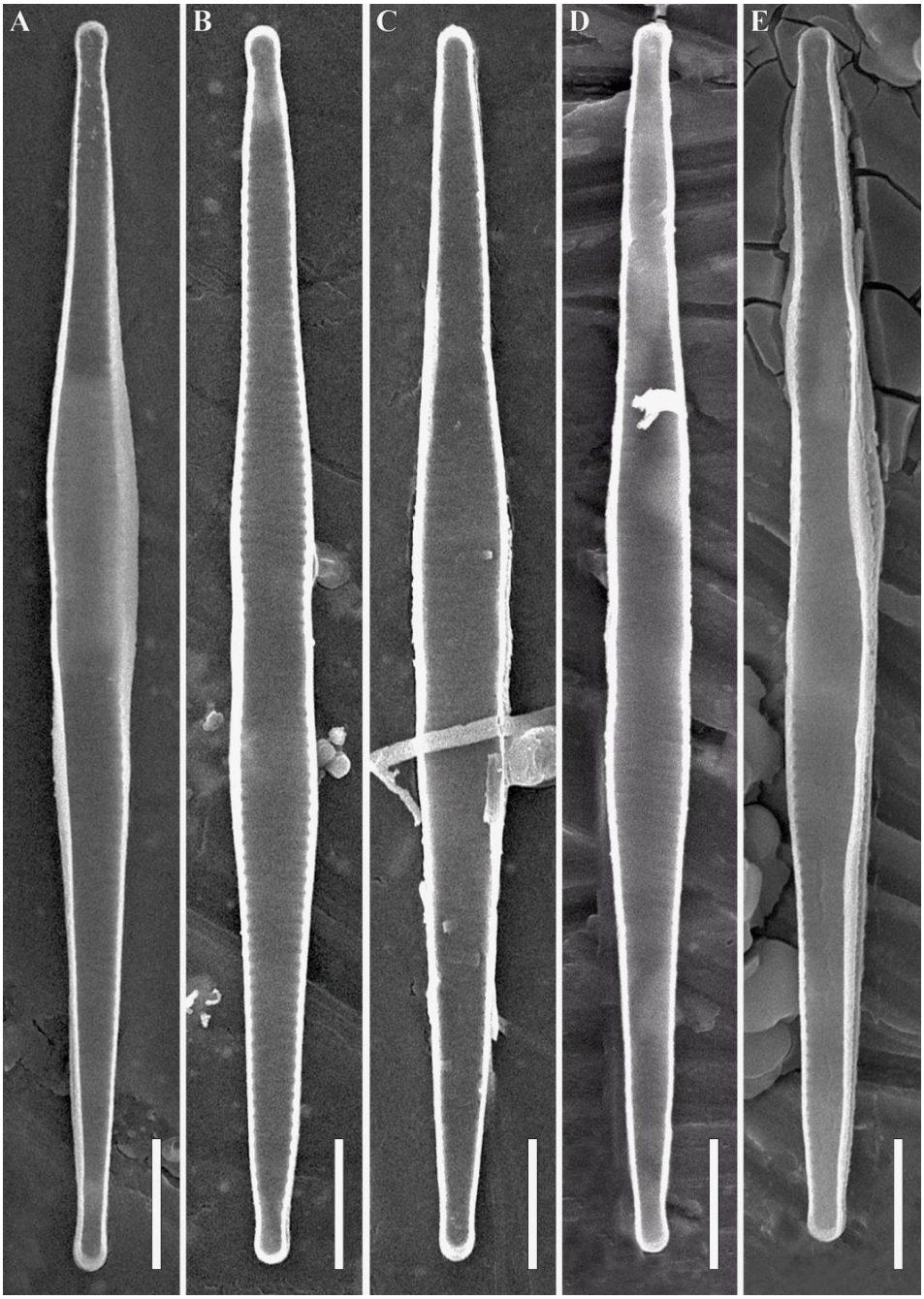

Figure 7. (**A**–**E**). *Fragilaria shirshovii* Glushchenko and Kulikovskiy sp. nov. Strain ARC 03. Scanning electron microscopy, internal views. The whole valve. Scale bars (**A**–**E**) = 5 μm.

Holotype here designated. Slide no. 08440 a (Figure 4F) from oxidized culture strain ARC 03, isolated in sample 3935, deposited in herbarium of MHA, Main Botanical Garden Russian Academy of Science, Moscow, Russia.

Isotype. Slide no. 08440 b, in Collection of Maxim Kulikovskiy at the Herbarium of the Institute of Plant Physiology Russian Academy of Science, Moscow, Russia.

Type locality. Russia, Kara Sea, Western Siberia, Gulf of Ob, 72°28.64′ N, 73°56.70′ E.

Representative specimens. Slides no. 08440 a, b and stub no. ARC 03 (oxidized material of culture strain ARC 03, isolated from sample no. 3935).

Etymology. Species dedicated to the renowned Russian hydrobiologist, the first researcher of Arctic phytoplankton, academician Pyotr Petrovich Shirshov (1905–1953).

Distribution. This species is known from the type locality.

PhycoBank registration: http://phycobank.org/103821 (accessed on 12 June 2023).

Description. LM (Figure 4A–W). Frustules in girdle view link with each other in the inflated central part, forming double comb-shaped colonies (Figure 4U,V). There is a structure in the form of two connected valves of different cells (Figure 4W). In valve view, valves are fusiform (in large specimens) to almost linear (in smaller specimens). The widest part of the valve has a variety of shapes. In large specimens, the central part is slightly swollen and then the valve margins become a little constricted, then expand again and finally narrow towards the valve ends (Figure 4A–P). In smaller specimens, more or less noticeable is only the slightly expanded central part (Figure 4Q–T). The ends are capitate in large specimens to subcapitate in smaller specimens (Figure 4A–T). The axial area is narrow lanceolate, with clear rounded or rectangular fascia at the central area. Ghost striae are present at the central area. The length is 30.4–47.8 μm and the width in the widest part is 3.1–3.7 μm. The striae alternate and are almost parallel (17–18 in 10 μm). Areolae are not discernible in LM.

SEM, external views (Figure 5A–F). The valve face is flat (Figure 5A–C). In the central part of the valve at the valve face/mantle junction, small flattened fragments of spatula-like spines (corroded or broken when separating the frustules during material preparation) are positioned (Figure 5A,C). In colonies, two valves of different frustules link together by spatula-shaped spines (Figure 5D). Closer to the valve ends at the valve face/mantle junction, small conical spines are positioned (Figure 5F). The spines are located both between the striae and on them (Figure 5A,C). Apical pore fields are composed of small poroids (Figure 5F, green arrow).

SEM, internal views (Figures 6A–F and 7A–E). Ghost striae are present at the central area (Figure 6D). The striae are noticeably narrower than the interstriae (Figure 6A–D). There is a single rimoportula per valve (Figures 6A–C and 7A–E). The rimoportulae are oriented at about 45° to the striae (Figure 6F,G). Apical pore fields are composed of small poroids and closed papillary outgrowths (Figure 6E–G). The lips of the rimoportula are well pronounced (Figure 6F,G). The striae are uniseriate and the areolae are small, rounded and 55–60 in 10 μm.

3.2. Molecular Analysis

To evaluate the phylogenetic position of the ARC 03 strain, we sequenced the highly variable V4 region of the ribosomal gene 18S rRNA and plastid gene *rbc*L. The sequenced genes selected for molecular analysis belonged to 35 diatom species and had a length of 1375 bp. The tree topology agreed well with the four-gene phylogram derived by Medlin et al. [37] for diatom araphid genera and the Bayesian phylogenetic tree based on the *rbc*L gene for *Fragilaria* taxa [16]. Phylogenetic analyses (BI, ML) with maximum sufficient statistical support (100 ML/100 BI) showed the affiliation of the ARC 03 strain to the genus *Fragilaria* (Figure 3). At the same time, inside this clade, ARC 03 occupies a related lineage for the s0327 strain of *F. bidens* Heiberg, *F. crotonensis* Kitton (TCC301 and AT 185Gel3) and *F. radians* (Kützing) D.M. Williams and Round (MM246 and ACH111).

4. Discussion

F. shirshovii sp. nov. is morphologically most similar to *F. crotonensis* Kitton sensu lato. Both species form comb-shaped colonies and the valves are linked by spatula-shaped spines in the central part (Table 1). The values of the valve width overlap are the following: 3.1–3.7 μm in *F. shirshovii* sp. nov. and 2–4(5) μm in *F. crotonensis* sensu auct. (Table 1). However, these two species clearly differ by the density of striae: 17–18 in 10 μm in *F. shirshovii* sp. nov. and 15–16 in 10 μm in *F. crotonensis* sensu stricto (Table 1). Previously, *F. crotonensis* was a catch-all taxon and many different taxa and populations were included to a broad concept of this species. As a result, the number of striae in different populations were detected as 14–19 in 10 μm (see Table 1). This broad range of striae needs clarification in the future under comprehensive investigations of different populations, including type population, using molecular and morphological investigations [14,18].

Table 1. Comparison of morphological features of *Fragilaria shirshovii* sp. nov. and related species.

	***F. shirshovii* sp. nov.**	***F. crotonensis* (Type Material)**	***F. crotonensis* (Sensu Auct.)**	***F. pararumpens***	***F. bidens***	***F. perminuta***
Colony formation	double comb-shaped	ribbon-like	ribbon- or comb-shaped	band-like aggregates, double comb-shaped	band-like	none
Outline	fusiform (in large specimens) to almost linear (in smaller specimens)	n.d.	narrowly lanceolate with proximal inflations, which can sometimes be constricted	rather narrow, lanceolate	linear	lanceolate or rhombic
Spines	spatula-shaped at the central part of the valve, small conical near the valve ends	n.d.	spatula-shaped at the central part of the valve, small conical near the valve ends	conical near the apex to spatulate in the middle	no data	absent
Valve ends	capitate in large specimens to subcapitate in smaller specimens	n.d.	subcapitate	subcapitate	wedge-shaped, often weakly protracted, bluntly to widely rounded	slightly rostrate
Axial area	narrow lanceolate	n.d.	in the form of very narrow sternum	absent	absent	absent
Central area	rounded or rectangular fascia	n.d.	rectangular hyaline zone	elliptic	rounded or rectangular fascia	strongly unilateral
Length, μm	30.4–47.8	45	40–170	25–50	10–50	7–40
Breadth, μm	3.1–3.7	n.d.	2–4(5)	2.5–3.5	(2)3–4	3–4
Striae in 10 μm	17–18	15–16	14–19	16–18	(11)15–18	17–21
Areolae per 10 μm	55–60	n.d.	composed of up to six apically elongated to almost rounded areolae	≈50	no data	60–65 [1]
Position of slit of rimoportula	about under 45° to striae	n.d.	oriented perpendicular to the striae, located in valve face or face/mantle junction	oriented almost parallel to the striae	no data	oriented almost parallel to the striae

Table 1. *Cont.*

	***F. shirshovii* sp. nov.**	***F. crotonensis* (Type Material)**	***F. crotonensis* (Sensu Auct.)**	***F. pararumpens***	***F. bidens***	***F. perminuta***
Habitat and ecology	This species is known from the type locality with the environmental conditions described in this study	n.d.	Despite intensive investigations, ecology amplitude is still not well defined, as differentiation from closely related forms in not straightforward. Mainly observed in mesotrophic, alkaline freshwater habitats with different electrolyte content. Eurythermic species.	Small, oligosaprobic running water and lakes on siliceous substrata	Alkaline meso- and strongly eutrophic waters	Calcium-bicarbonate-rich, meso- to moderately eutrophic lakes. Usually absent from more strongly eutrophic and saprobically impacted freshwater habitats.
References	This study	[18]	[14,18,38]	[12,35,36]	[39–42]	[12,15,34]

[1] counted by us from published data, n.d.–no data. The lips and inner opening of rimoportula in *F. shirshovii* sp. nov. are located on the valve face at an angle to the terminal striae at the ends of the valves (Figure 6F,G). In *F. crotonensis,* the lips and inner opening are oriented perpendicular to the striae and the opening can be located either on the valve face or valve margin [18].

The important difference between *F. shirshovii* sp. nov. and *F. crotonensis* is the valve shape (Table 1).

F. shirshovii sp. nov. is similar to *F. pararumpens* according to Lange-Bertalot, Hofmann and Werum in Hoffmann et al. in 2011, primarily in terms of the shape of the colonies. The valves of *F. shirshovii* sp. nov. (Figure 4U,V) and *F. pararumpens* are connected in the central part, forming the so-called ribbon-like double comb-shaped colonies [18]. The differentiation of the spine shape in the central parts of the valve and at the valve ends is also similar in these species; there are conical spines at the valve ends and spatula-shaped spines in the central part (Table 1). The valve width in the two species overlaps (3.1–3.7 µm in *F. shirshovii* sp. nov. vs. 2.5–3.5 µm in *F. pararumpens*), as well as striae density (17–18 in 10 µm in *F. shirshovii* sp. nov. vs. 16–18 in 10 µm in *F. pararumpens*). The rimoportula in both *F. shirshovii* sp. nov. and *F. pararumpens* is oriented at about a 45° angle to the striae (Table 1) [35]. Nevertheless, these two species are distinctly different morphologically. The central part of the valve is shaped differently; *F. shirshovii* sp. nov. has a less pronounced central inflation that transitions into the further widening of the valve edges (Figure 4A–P), whereas in *F. pararumpens*, the central inflation is usually more distinct [36]. Areolae density is higher in *F. shirshovii* sp. nov. than in *F. pararumpens* (55–60 in 10 µm in *F. shirshovii* sp. nov. vs. 50 in 10 µm in *F. pararumpens*).

F. bidens Heiberg 1863 (used name—*F. rhabdosoma* Ehrenberg 1833) has a rounded inflation in the central part of the valve similar to *F. shirshovii* sp. nov. [39–42]. These species also have a similar valve width (3.1–3.7 µm in *F. shirshovii* sp. nov. vs. 3–4 µm in *F. bidens*) and striae density (17–18 in 10 µm in *F. shirshovii* sp. nov. vs. 15–18 in 10 µm in *F. bidens*). The valve ends in the smaller specimens of *F. bidens* are blunter than in similarly sized valves of *F. shirshovii* sp. nov. (Table 1). The central inflation in the small specimens of *F. bidens* is more pronounced [39,40] than in the small specimens of *F. shirshovii* (Figure 1P–T).

F. shirshovii sp. nov. is similar to *F. perminuta* (Grunow) Lange-Bertalot 2000 only in valve width and striae density (Table 1). *F. perminuta* does not form colonies and lacks spines on its valves, while *F. shirshovii* sp. nov. cells are linked by their spines in comb-shaped colonies (Figures 4–6). The valve shape is also different; *F. shirshovii* sp. nov. has fusiform to almost linear valves whereas *F. perminuta* has lanceolate to rhombic valves [15,34]. The central area in *F. shirshovii* sp. nov. is rounded to rectangular (Figure 4A–T), and in *F. perminuta*, it is strongly one-sided [15,34]. The rimoportula in *F. shirshovii* sp. nov. is oriented at about a 45° angle to the striae (Table 1), and in *F. perminuta*, the rimoportula is almost parallel to the striae [15].

Author Contributions: Conceptualization, M.S.K.; investigation, methodology, N.V.L. and A.M.G.; sampling, N.V.L.; morphology investigation, A.M.G., S.I.G. and M.S.K.; molecular investigation, N.V.L. and Y.I.M.; funding acquisition, N.V.L.; writing—original draft preparation, A.M.G. and N.V.L.; writing—review and editing, N.V.L., A.M.G., Y.I.M. and M.S.K. All authors have read and agreed to the published version of the manuscript.

Funding: The work was carried out within the framework of the Russian Science Foundation (project no. 22-24-00945).

Institutional Review Board Statement: Not applicable.

Data Availability Statement: Date in this article.

Acknowledgments: We are grateful to the staff of the Center of Electron Microscopy of the Papanin Institute for Biology of Inland Waters, RAS, for their technical assistance (Figures 5 and 6). We also thank Alexey V. Shapagin (Laboratory of Structural and Morphological Research, Frumkin Institute of Physical Chemistry and Electrochemistry, Russian Academy of Sciences, Moscow, Russia) for his invaluable help in obtaining the images presented in Figure 7. We wish to thank the "Floating University" scientific and educational program for their support in the organization of field measurements.

Conflicts of Interest: The authors declare no conflict of interest.

References

1. Carmack, E.C.; Yamamoto-Kawai, M.; Haine, T.W.N.; Bacon, S.; Bluhm, B.A.; Lique, C.; Melling, H.; Polyakov, I.V.; Straneo, F.; Timmermans, M.L. Freshwater and its role in the Arctic Marine System: Sources, disposition, storage, export, and physical and biogeochemical consequences in the Arctic and global oceans. *J. Geophys. Res. Biogeosci.* **2016**, *121*, 675–717. [CrossRef]
2. Flint, M.V.; Poyarkov, S.G.; Rimsky-Korsakov, N.A. Ecosystems of the Russian Arctic-2015 (63rd Cruise of the research vessel Akademik Mstislav Keldysh). *Oceanology* **2016**, *56*, 459–461. [CrossRef]
3. PAME. *Working Group on the Protection of the Arctic Marine Environment. Report to the Third Ministerial Conference on the Protection of the Arctic Environment, Norwegian Ministry of Environment*; PAME: Oslo, Norway, 1996.
4. Flint, M.V. Cruise 54th of the research vessel Akademik Mstislav Keldysh in the Kara Sea. *Oceanology* **2010**, *50*, 637–642. [CrossRef]
5. Polyakov, I.; Walsh, D.; Dmitrenko, I.; Colony, R.L.; Timokhov, L.A. Arctic ocean variability derived from historical observations. *Geophys. Res. Lett.* **2003**, *30*, 1298. [CrossRef]
6. Polyakov, I.V.; Alexeev, V.A.; Belchansky, G.I.; Dmitrenko, I.A.; Ivanov, V.V.; Kirillov, S.A.; Korablev, A.A.; Steele, M.; Timokhov, L.A.; Yashayaev, I. Arctic Ocean Freshwater Changes over the Past 100 Years and Their Causes. *J. Clim.* **2008**, *21*, 364–384. [CrossRef]
7. Dittmar, T.; Kattner, G. The biogeochemistry of the river and shelf ecosystem of the Arctic Ocean: A review. *Mar. Chem.* **2003**, *83*, 103–120. [CrossRef]
8. Kaika, M. The Water Framework Directive: A New Directive for a Changing Social, Political and Economic European Framework. *Eur. Plan. Stud.* **2003**, *11*, 299–316. [CrossRef]
9. Lobus, N.V.; Kulikovskiy, M.S. The Co-Evolution Aspects of the Biogeochemical Role of Phytoplankton in Aquatic Ecosystems: A Review. *Biology* **2023**, *12*, 92. [CrossRef]
10. Kelly, M.; Boonham, N.; Juggins, S.; Kille, P.; Mann, D.; Pass, D.; Sapp, M.; Sato, S.; Glover, R.; Walsh, K. *A DNA Based Diatom Metabarcoding Approach for Water Framework Directive Classification of Rivers*; Environment Agency: Bristol, UK, 2018; ISBN 978-1-84911-406-6.
11. Wang, X.; Zheng, B.; Liu, L.; Li, L. Use of Diatoms in River Health Assessment. *Annu. Res. Rev. Biol.* **2014**, *4*, 4054–4074. [CrossRef]
12. Lange-Bertalot, H.; Hofmann, G.; Werum, M.; Cantonati, M. *Freshwater Benthic Diatoms of Central Europe: Over 800 Common Species Used in Ecological Assessment*; Koeltz Botanical Books: Stuttgart, Germany, 2017.
13. Su, Y.; Lundholm, N.; Ellegaard, M. Effects of abiotic factors on the nanostructure of diatom frustules—Ranges and variability. *Appl. Microbiol. Biotechnol.* **2018**, *102*, 5889–5899. [CrossRef]
14. Kulikovskiy, M.S.; Glushchenko, A.M.; Genkal, S.I.; Kuznetsova, I.V. *Identification Book of Diatoms from Russia*; Filigran: Yaroslavl, Russia, 2016; ISBN 978-5-906682-72-7.
15. Kahlert, M.; Kelly, M.G.; Mann, D.G.; Rimet, F.; Sato, S.; Bouchez, A.; Keck, F. Connecting the morphological and molecular species concepts to facilitate species identification within the genus *Fragilaria* (Bacillariophyta). *J. Phycol.* **2019**, *55*, 948–970. [CrossRef]
16. Zakharova, Y.; Marchenkov, A.; Petrova, D.; Bukin, Y.; Morozov, A.; Bedoshvili, Y.; Podunay, Y.; Davidovich, O.; Davidovich, N.; Bondar, A.; et al. Delimitation of Some Taxa of *Ulnaria* and *Fragilaria* (Bacillariophyceae) Based on Genetic, Morphological Data and Mating Compatibility. *Diversity* **2023**, *15*, 271. [CrossRef]
17. Sukhanova, I.N.; Flint, M.V.; Mosharov, S.A.; Sergeeva, V.M. Structure of the phytoplankton communities and primary production in the Ob River estuary and over the adjacent Kara Sea shelf. *Oceanology* **2010**, *50*, 743–758. [CrossRef]
18. Lange-Bertalot, H.; Ulrich, S. Contributions to the taxonomy of needle-shaped *Fragilaria* and *Ulnaria* species. *Lauterbornia* **2014**, *78*, 1–73.
19. Krammer, K.; Lange-Bertalot, H. Bacillariophyceae 3. Teil: Centrales, Fragilariaceae, Eunotiaceae. In *Suβwasserflora von Mitteleuropa*; Ett, H., Gerloff, J., Heynig, H., Mollenhauer, D., Eds.; Gustav Fischer: Stuttgart, Germany, 1991; Volume 2, p. 598.
20. Pavlov, V.K.; Timokhov, L.A.; Baskakov, G.A.; Kulakov, M.Y.; Kurazhov, V.K.; Pavlov, P.V.; Pivovarov, S.V.; Stanovoy, V.V. *Hydrometeorological Regime of the Kara, Laptev, and East-Siberian Seas*; Washington University Seattle Applied Physics Lab, USA: Seattle, WA, USA, 1996.
21. Osadchiev, A.; Konovalova, O.; Gordey, A. Water Exchange between the Gulf of Ob and the Kara Sea during Ice-Free Seasons: The Roles of River Discharge and Wind Forcing. *Front. Mar. Sci.* **2021**, *8*, 741143. [CrossRef]
22. Lobus, N.V.; Glushchenko, A.M.; Osadchiev, A.A.; Maltsev, Y.I.; Kapustin, D.A.; Konovalova, O.P.; Kulikovskiy, M.S.; Krylov, I.N.; Drozdova, A.N. Production of Fluorescent Dissolved Organic Matter by Microalgae Strains from the Ob and Yenisei Gulfs (Siberia). *Plants* **2022**, *11*, 3361. [CrossRef] [PubMed]
23. Sazhin, A.F.; Romanova, N.D.; Mosharov, S.A. Bacterial and primary production in the pelagic zone of the Kara Sea. *Oceanology* **2010**, *50*, 759–765. [CrossRef]
24. Guillard, R.R.L.; Lorenzen, C.J. Yellow-green algae with chlorophyllide $c^{1,2}$. *J. Phycol.* **1972**, *8*, 10–14. [CrossRef]
25. Andersen, R.A.; Masanobu, K. Microalgae Isolation Techniques. In *Algal Culturing Techniques*; Andersen, R.A., Ed.; Elsevier Inc.: Amsterdam, The Netherlands, 2005; p. 578, ISBN 0-12-088426-7.
26. Zimmermann, J.; Jahn, R.; Gemeinholzer, B. Barcoding diatoms: Evaluation of the V4 subregion on the 18S rRNA gene, including new primers and protocols. *Org. Divers. Evol.* **2011**, *11*, 173–192. [CrossRef]
27. Ruck, E.C.; Theriot, E.C. Origin and Evolution of the Canal Raphe System in Diatoms. *Protist* **2011**, *162*, 723–737. [CrossRef]

28. Daugbjerg, N.; Andersen, R.A. A molecular phylogeny of the heterokont algae based on analyses of chloroplast encoded rbcL sequence data. *J. Phycol.* **1997**, *33*, 1031–1041. [CrossRef]
29. Kumar, S.; Stecher, G.; Tamura, K. MEGA7: Molecular Evolutionary Genetics Analysis Version 7.0 for Bigger Datasets. *Mol. Biol. Evol.* **2016**, *33*, 1870–1874. [CrossRef]
30. Katoh, K.; Toh, H. Parallelization of the MAFFT multiple sequence alignment program. *Bioinformatics* **2010**, *26*, 1899–1900. [CrossRef] [PubMed]
31. Drummond, A.J.; Rambaut, A. BEAST: Bayesian evolutionary analysis by sampling trees. *BMC Evol. Biol.* **2007**, *7*, 214. [CrossRef]
32. Darriba, D.; Taboada, G.L.; Doallo, R.; Posada, D. jModelTest 2: More models, new heuristics and parallel computing. *Nat. Methods* **2012**, *9*, 772. [CrossRef]
33. Stamatakis, A.; Hoover, P.; Rougemont, J. A Rapid Bootstrap Algorithm for the RAxML Web Servers. *Syst. Biol.* **2008**, *57*, 758–771. [CrossRef] [PubMed]
34. Delgado, C.; Novais, M.H.; Blanco, S.; de Almeida, S.F.P. Examination and comparison of *Fragilaria candidagilae* sp. nov. with type material of *Fragilaria recapitellata*, *F. capucina*, *F. perminuta*, *F. intermedia* and *F. neointermedia* (Fragilariales, Bacillariophyceae). *Phytotaxa* **2015**, *231*, 1–18. [CrossRef]
35. Heudre, D.; Wetzel, C.E.; Moreau, L.; Van de Vijver, B.; Ector, L. On the identity of the rare *Fragilaria subconstricta* (Fragilariaceae), with *Fragilaria* species forming ribbon-like colonies shortly reconsidered. *Plant Ecol. Evol.* **2019**, *152*, 327–339. [CrossRef]
36. Van de Vijver, B.; Schuster, T.M.; Williams, D.M.; Kusber, W.H. Was *Fragilaria pararumpens* Lange-Bertalot, G. Hofmann & Werum 2011 new to science? *Not. Algarum* **2021**, *180*, 1–4.
37. Medlin, L.; Yang, I.; Sato, S. Evolution of the Diatoms. VII. Four gene Phylogeny assesses the validity of selected araphid genera. *Nov. Hedwigia* **2012**, *141*, 505–513.
38. Alexson, E.E.; Reavie, E.D.; Van de Vijver, B.; Wetzel, C.E.; Ector, L.; Wellard Kelly, H.A.; Aliff, M.N.; Estepp, L.R. Revision of the needle-shaped *Fragilaria* species (Fragilariaceae, Bacillariophyta) in the Laurentian Great Lakes (United States of America, Canada). *J. Great Lakes Res.* **2022**, *48*, 999–1020. [CrossRef]
39. Kulikovskiy, M.S.; Genkal, S.I.; Mikheyeva, T.M. New Data for the Bacillariophyta Flora of Belarus. 1. Family Naviculaceae Kütz. *Int. J. Algae* **2010**, *12*, 37–56. [CrossRef]
40. Bąk, M.; Witkowski, A.; Żelazna-Wieczorek, J.; Wojtal, A.Z.; Szczepocka, E.; Szulc, K.; Szulc, B. *Klucz do Oznaczania Okrzemek w Fitobentosie na Potrzeby Oceny Stanu Ekologicznego Wód Powierzchniowych w Polsce*; Biblioteka Monitoringu Środowiska: Warszawa, Poland, 2012.
41. Chudaev, D.A.; Gololobova, M.A. *Diatoms of the Glubokoe Lake (Moscow Region)*; KMK: Moscow, Russia, 2016.
42. Bazhenova, O.P.; Glushchenko, A.M.; Igoshkina, I.Y.; Shkilev, T.E.; Kulikovskiy, M.S. Plankton diatoms (Fragilariophyceae, Bacillariophyceae) from the middle part of Irtysh River. *Nov. Sist. Nizshikh Rastenii* **2019**, *53*, 207–240. [CrossRef]